# THE USE OF QUANTITATIVE FRACTOGRAPHY IN FATIGUE CRACK GROWTH STUDIES

B. Karlsson* and J. Wasén*

Fatigue crack surfaces generally have a stochastic character requiring statistical descriptions. The simple distributions often found are conveniently characterized by means and standard deviations. The fracture surfaces are effectively described by angle distributions, height distributions, and spatial descriptors. Such distributions develop during the fracture process as a result of the complicated interaction between the local stress field and the stochastic microstructure at the crack front. Fractographic data from various one- and two-phase steels are reviewed and related to the underlying microstructure. For instance it is demonstrated that the crack closure stress intensity $K_{cl}$ is proportional to the power 1/3 of the mean standard deviation of height $\bar{H}$.

## INTRODUCTION

Awareness of the importance of the crack geometry for the fatigue crack growth has gradually developed during recent years. For instance, this has lead to the development of models for the growth rate. However, the experimental and theoretical tools to quantify the geometry of non-planar surfaces have only recently reached a state where more realistic descriptors are available. In addition, until now very little experimental information on the geometrical character of fracture surfaces has been available in the literature. In the present paper techniques for computerized fracture profile analysis developed in the authors' laboratory are described. These techniques contain detailed procedures for geometrical evaluations of the fracture surfaces. The geometrical descriptors used rely on the fact that the fracture surfaces develop in a stochastic manner, ruling out the geometrically regular models used by various investigators. A systematic overview is given over the various descriptors developed so far for describing fracture surfaces. Relevant geometrical variables are identified allowing a precise correlation between the stochastic fracture

* Department of Engineering Metals, Chalmers University of Technology, S-412 96 Göteborg, Sweden

events and the underlying microstructure. The experimental information is based on data taken from various one-phase and two-phase steels. The linear size is of the constituents has been varied in the range 5 to 100 $\mu$m.

The relevance of different geometrical discriptors must be judged from their possibility to be connected to microstructural quantities. In addition such parameters should allow connections to the crack growth characteristics like crack closure, crack growth threshold levels and crack propagation rates. Such demands have hardly been met by the techniques available in the past. Qualitative, although detailed, fractographic descriptions have more been used to identify specific features in the fracture surfaces with little possibility to quantitative predictions of the fatigue crack growth behaviour.

The geometrical situation is schematically shown in fig. 1, indicating the non-planar fracture surface as well as a projection of the surface and a section (profile) through it. Direct viewing in a single direction, as employed in conventional SEM techniques, only permits qualitative evaluations of details in the fracture surface. Still, relatively flat surfaces like grain boundary facets and transcrystalline cleavage allow approximate determinations of the true surface geometry. A more exact account of the non-planar geometry requires stereoscopical recordings where image pairs with known tilt angles are used. Photogrammatical evaluation of such image pairs is then performed enabling a reconstruction of the spatial coordinates in the original fracture surface. The recording of such coordinates is operator demanding and permits only relatively few coordinates to be evaluated (Bauer and Haller (1)). The application of automatic image analyzers is developing but still very limited due to substantial difficulties in finding reliable contrast and discrimination methods; further the need for large computer capacity is still an impeding factor (e.g. Paul et al. (2)). A more fundamental problem in stereometry is the shadowing effects occurring on overlapping or highly rugged surfaces. From a fractographical point of view the most serious limitation with this technique is the lack of microstructural, subsurface information needed to interpret the fractographic behaviour. The drawbacks of the non-destructive stereoscopical techniques are largely eliminated by coordinate analysis on fracture profiles taken from vertical sections through the fracture surface (e.g. Wright and Karlsson (3), Banerji and Underwood (4)). Conventional metallographical preparation techniques followed by digitizing of the profile (directly in the metallographic mount or on photographs) then permit quantitative analysis of the profile in relation to the underlying microstructure. Overlapping is no problem in the profile analysis. In practice, computer support is necessary in both stereometry and profile analysis. The geometrical evaluations are basically the same in the two cases.

The fracture surfaces can be described by roughness indices

like the linear rougness index and the surface roughness index (e.g. Wright and Karlsson (3)). These indices are related to each other and they constitute one-parametric descriptions of the surface geometry. A more complete characterization requires determination of the angular distributions of linear and areal elements, which in a realistic manner geometrically describe the fracture process. Further, the height distribution which incorporates both the size scale and the angular properties of the fracture surface is a very valuable descriptor of the surface. Finally, the spatial characteristics like Fourier series and fractal curves describe essential properties of the geometry. These different methods are complementary and no single one can replace the others. It should be emphasized that profile analysis in particular permits analysis of fracture paths through individual phases in multiphase materials. A problem experienced in most fractographic studies is the presence of long-waved irregularities in the fracture profile, making averaging and evaluation of the height distribution very hard. Such irregularities reflect a fundamental property of the fracture process. By the use of filtering techniques this difficulty can be overcome and a transformed surface can be created where a more direct comparison between for instance the height distribution and the microstructure is facilitated.

## BASIC APPROACHES

The quantitative description of fracture surfaces is basically a problem of characterizing non-planar, localized surfaces. Classical stereology (Underwood (5)) has developed techniques to measure and quantify uniformly distributed surfaces. One usually assumes a uniform orientation of the normals to the surface elements (random normal orientation, RNO). The standard use of straight test lines to determine the surface density of uniformly distributed RNO surfaces is only to a limited extent applicable for localized surfaces (Wright and Karlsson (3)). Attempts to extend this idea by combining surface elements with partly RNO, partly flat surface elements (Coster and Chermant (6)) do not seem to widen the applicability of this kind of surface models. In fact, such surface representations seem unable to create an understanding of the real fracture processes and their relation to the microstructure.

The microstructure in single-phase or poly-phase materials often controls the propagating crack. This may be due to inherent effects of the microstructure itself or may result from the extension and shape of the strain field at the crack tip. The exact geomety of the fracture surface is therefore rather complicated and in general not simply foreseeable from the microstructure.

Basically the fracture surface (and thus the fracture profile) has a stochastic or nonperiodic character. This irregularity has its roots in the local fracture events at the crack tip as well as in the nonrepetitive geometry of the microstructure. An

additional reason may be nonsymmetries in the loaded specimens, even though the results of this paper clearly emphasize the former factors as being decisive. A consequence of such a fracture behaviour is that the fracture surface can be described only by geometrical distributions (mean values and deviations). The surface distribution in space is then conveniently described by the following quantities:

(i) Angle distributions or roughness indices.
(ii) Fracture element size distributions.
(iii) Surface height distributions.
(iv) The spatial distribution as represented by the wavelengths (frequencies) of the fracture surface or by equivalent measures such as the fractal properties.

The analysis in this paper is mainly performed on profile contours. General evaluations of the surface quantities are possible in some cases; in others nonsymmetry limitations makes the transformation to three-dimensional parameters more difficult.

## DEFINITION OF A REFERENCE SURFACE (LINE). DATA RECORDING

A problem in the profile or surface analysis is that a long-waved irregularity sometimes appears (Park and Fine (7), Wasén et al. (8)) and overlays the local fracture geometry (fig. 2). A method to suppress non-averaged information from the measurements in order to get a suitable measure of the local, microstructurally induced roughness is to use a digital high pass filter technique (Wasén et al. (8)). This technique uses a Fourier transformation of the crack profile from a length series to a frequency series, followed by cut-off of the low frequencies (i.e. the long-waved irregularity), and finally an inverse Fourier transformation of the remaining frequencies back to a length series.

The Fourier spectrum is suitably referred to a straight regression line based on the digitized points ("zero level" in fig. 2). In the filtering, the cut-off frequency can be chosen according to a geometric criterion, for example a frequency corresponding to a certain macroscopic irregularity; alternatively a microstructurally determined criterion can be used. In fig. 2, for instance, 50 grains were chosen as the cut-off wavelength. The reference line is then identified with the filtered low-frequency (long wavelength) part and follows the macroscopic irregularity (fig. 2). Further details on the filtering technique have been discussed by Wasén et al. (8).

The two major arguments for the use of filtering are the following: Firstly, the width of the height distribution should not much exceed the grain size (or a corresponding, relevant microstructural unit), and secondly a comparatively short line of analysis allows a good averaging to be attained. A detailed analysis

(Wasén et al. (8)) on real fractographs has shown that the height distribution is strongly sensitive to the filtering out of the waviness whereas the angular distribution is rather insensitive to this procedure (cf. the scales of the profile in fig. 2). Analytical results reported elsewhere (Wasén and Karlsson (9)) indicate that the probability of finding the unfiltered crack outside the main fracture plane can be quantitatively predicted in terms of the microstructure. Such results reflect the stochastic crack growth behaviour and demonstrate the necessity of using filtering in the evaluation of the height distribution.

In the experimental recordings, the fracture profile is digitized with a resolution of 0.5 $\mu$m. The coordinates for the Fourier transformation are produced in the following manner: The x-coordinates (with desired spacings) are selected by equidistant stepping along the regression line and the corresponding y-coordinates are calculated by successive regression based on the three nearest input points (Bengtsson et al. (10)) causing reduction of irrelevant "noise" introduced by the digitizing procedure (Wasén et al. (8)). Thereby the "real" profile is represented by new coordinates accurately following the fracture surface and defining the line of analysis.

The resolution in the digitizing procedure should be determined by the degree of detailed information needed to quantify the surface in a proper way. In the experimental cases referred below the resolution needed is of the order of a few per cent of the grain size. However, the evaluation techniques described are quite general and are applicable at any resolution level.

## ANGULAR DISTRIBUTIONS

The angle distribution of a profile, i.e. the distribution of angles between the chords approximating the fracture profile and the reference line, can conveniently be described by weighting against the relative chord lengths along the the profile line. Experimental data on fracture profiles in single phase materials often reveal Gaussian distributions truncated at $\pm 90^{\circ}$ (fig. 3). A suitable measure of the "average" local crack direction is then provided by the standard deviation, $\bar{\theta}_L$, of the angle distribution $f(\theta_L)$. The distribution function and its standard deviation is then effectively described by the following relations:

$$f(\theta_L) = \left\{ e^{-[\theta_L^2/(2\sigma^2)]} \right\} / \left\{ \int_{-90^{\circ}}^{90^{\circ}} e^{-[\theta_L^2/(2\sigma^2)]} d\theta_L \right\} \qquad (1a)$$

where $-90^{\circ} \leq \theta_L \leq 90^{\circ}$

$$\overline{\theta}_L^2 = \int_{-90^o}^{90^o} \theta_L^2 \cdot f(\theta_L) d\theta_L \qquad (1b)$$

The shape of the distribution function $f(\theta_L)$ is determined by the $\sigma$-value. Due to the truncation at $\pm 90^o$, this shape gradually changes from that of a normal distribution to that of a RNO distribution upon increasing $\sigma$. The relation between $\sigma$ and the standard deviation $\overline{\theta}_L$ of $f(\theta_L)$ is shown in fig. 4. Note that, because of the truncation, $\overline{\theta}_L$ can be used as an approximation of $\sigma$ only for relatively small values of $\overline{\theta}_L$ (cf. fig. 4).

An alternative way to describe the linear angle distribution is to weight against the relative lengths along the reference line (i.e. approximately along the main crack direction). Such a distribution is analytically related to eqs. 1a and 1b and has been described by Karlsson et al. (11).

Area weighted angle distributions used as surface descriptors are of interest, for instance in showing the orientation of fracture surface elements in relation to the principal stress direction. So far no general theory seems to exist for the conversion of linear angle distributions to corresponding surface angle distributions. For the case of rotational symmetry around the normal to the reference fracture plane (approximately parallel to the principal stress direction) such conversion functions have been derived (Davies and Wilshire (12), Scriven and Williams (13)). These conversion formulae are expressed as equivalent multiplying factors for a stepwise transformation of the linear to the surface angle distributions.

In the conversion procedure the angle distribution of the length elements is grouped into n classes with a class width $h = 90^o/n$. The corresponding distribution function F(i,h) is defined so that F(i=1,h) answers to the interval $90^o\text{-}h < \theta_L \leq 90^o$ and F(i=n,h) to $0 \leq \theta_L \leq h$. The multipliers $k_{ji}$ (eq. 2c) allow the accompanying distribution function G(j,h) (eq. 2a) of the surface normals to be evaluated, where j=1 corresponds to the smallest angles found in the interval $0 \leq \theta_S \leq h$.

$$G(j,h) = S(j,h) - S((j-1),h) \qquad j = 1,2,3,\ldots,n \qquad (2a)$$

$$S(j=0,h) = 0$$

$$S(j,h) = \left\{ \sum_{i=1}^{j} (k_{ji} \cdot F(i,h)) \right\} / \left\{ \sum_{i=1}^{n} (F(i,h)) \right\} \qquad (2b)$$

$$k_{ji} = \frac{\sin(j \cdot h)}{h} \cdot \left\{ \sin^{-1}\left[\frac{\sin(i \cdot h)}{\sin(j \cdot h)}\right] - \sin^{-1}\left[\frac{\sin((i-1) \cdot h)}{\sin(j \cdot h)}\right] \right\} \qquad (2c)$$

By the aid of these conversion formulae any kind of linear angle distribution can be transfered to the corresponding area weighted angle distribution. For instance, assumed truncated Gaussian distributions $f(\theta_L)$ according to eq. 1a lead to corresponding surface normal distributions $g(\theta_S)$ as shown in fig. 5. Application of this technique to the linear angle distribution $f(\theta_L)$ in fig. 3 - originating from the experimental fracture profile in fig. 2 - leads to an area weighted angle distribution $g(\theta_S)$ (fig. 3) much resembling the synthesized distributions in fig 5.

Experimental measurements on profiles taken parallel to and perpendicular to the main crack propagation direction in various one- and two-phase steels have shown that the assumption of rotational symmetry is reasonably well fulfilled (Karlsson et al. (11). Therefore, the use of these transformation formulae is certified. Experimental recordings of a variety of fatigue fracture profiles in the authors' laboratory (Karlsson et al. (11)) indicate that the linear angle distribution fairly well can be represented by truncated Gaussian distributions (eq. 1a) with various magnitudes of the standard variation $\bar{\theta}_L$. For instance, the fairly smooth fracture profiles found in pearlitic structures show typically $\bar{\theta}_L \approx 15^o$ (Hamberg et al. (14)), whereas the extremely rugged fracture surfaces found in porous, sintered steels correspond to $\bar{\theta}_L \approx 45^o$ (Bertilsson and Karlsson (15)). A comparison with fig. 5 indicates that a "flat" surface has a rather narrow area weighted angle distribution with a maximum value at low angles. Rougher surfaces, on the other hand, correspond to a broader distributions $g(\theta_S)$ with less marked peak values.

Theoretical calculations on truncated, Gaussian linear angle distributions as well as experimental information show approximately a proportionality between $\bar{\theta}_L$ and the arithmetic mean value of the area weighted angle distribution, $\theta_{Sm}$ (fig. 6):

$$\theta_{Sm} \approx 1.15 \cdot \bar{\theta}_L \qquad (3)$$

## ROUGHNESS INDICES

A simplified approach to the description of surface orientations is to use roughness indices as averaging parameters of the angular distributions. The most commonly used rougness indices refer to profile lines and surfaces respectively (Wright and Karlsson (3), Underwood (16)). Thus the linear and surface roughness indices $R_L$ and $R_S$ are defined according to the following formulae:

$$R_L = l / l' \qquad (4a)$$

and

$$R_S = S / S' \qquad (4b)$$

where l and S denote the total line length and surface area respectively and l' and S' refer to the projected quantities on the reference line (surface). These roughness indices can be expressed in a more general way by a direct connection to the line and area weighted angle distributions:

$$R_L = \left\{ \int_{-90^o}^{90^o} f(\theta_L) d\theta_L \right\} / \left\{ \int_{-90^o}^{90^o} f(\theta_L) \cdot \cos(\theta_L) d\theta_L \right\} \quad (5a)$$

$$R_S = \left\{ \int_{-90^o}^{90^o} g(\theta_S) d\theta_L \right\} / \left\{ \int_{-90^o}^{90^o} g(\theta_S) \cdot \cos(\theta_S) d\theta_L \right\} \quad (5b)$$

Application of these formulae on the truncated, Gaussian linear angle distributions in eq. 1a and the corresponding area weighted angle distributions (of type shown in fig. 5) leads to roughness values as displayed in fig. 6. Various attempts have been made to develop quantitative relations between $R_L$ and $R_S$. The first referred to here (eq. 6a) is based on a simple surface step model but has proven as an accurate predictor also for various random-type surfaces (Wright and Karlsson (3)):

$$R_S^* = 1 + \pi/2 \cdot (R_L - 1) \quad (6a)$$

Previous tests (Wright and Karlsson (3)) have shown that this relation underestimates $R_S$ by approximately 5 % at large $R_L$ with progressively better accuracy at smaller $R_L$. The same deviation is found when a comparison is made with the results in fig. 6. An alternative relation has been proposed by Underwood (16):

$$R_S^{**} = 1 + 4/\pi \cdot (R_L - 1) \quad (6b)$$

This relation is less useful as it underestimates $R_S$ by roughly 15 % at large $R_L$ - values, again with better accuracy at smaller $R_L$. These estimations of the accuracy of eqs. 6a and 6b are further supported by the analytically known results from RNO-surfaces (Wright and Karlsson (3)).

The $R_S$-value can for instance be used to express true mean feature characteristics as linear size, perimeter lengths and interdistances from the corresponding quantities measured on single projections (e.g. Underwood (17)). For this purpose the $R_S$-$R_L$ relations in eqs. 6a and 6b can be used, starting from experimental data from the fracture profile.

The roughness indices $R_L$ and $R_S$ can sometimes be used as alternatives to the "mean" values $\bar{\theta}_L$ and $\theta_{Sm}$ of the angle distributions (eqs. 1 and 3; fig. 6). For fracture mechanical interpretations and modelling the representation with angles is much to be

preferred.

## FRACTURE ELEMENT SIZE DISTRIBUTIONS

Studies on fracture profiles in ferritic (Wasén et al. (18)) and pearlitic (Hamberg (19)) steels have indicated that the fracture surface can be approximated with a pattern of sequential facets of different sizes and orientations. Each facet appears as a result of a stochastic fracture process governed by certain probailities for the size and orientation. Accordingly, the digitized profile can with good accuracy be approximated by a coarser chord chain between the deflection points in the fracture path. The same kind of fracture behaviour has also been found in WC-Co alloys (Sigl and Exner (20)). It should be emphasized that such a profile approximation does not markedly influence the angle and height distributions.

An analysis of the fracture profile in single phase ferrite as shown in fig. 2 lead to the chord length distribution displayed in fig. 7. This distribution can reasonably well be represented by a log-normal distribution $N_{\log}[\bar{l},\sigma_l]$. Further investigations on crack profiles from ferritic steels have indicated a linear relation between the grain size and the mean linear fracture element size $\bar{l}$ (Wasén et al. (18)). The logarithmic standard deviation $\sigma_l$ of the length distributions was found to be 0.6-0.7 and independent of the grain size. This standard deviation coincides fairly well with the deviation of the log-normally distributed linear grain intercepts (Woodhead (21)).

Information on the relation between the chord length distribution and the underlying microstructure in two-phase materials is still fairly limited. Nevertheless, the sized of these chords are believed to be uniquely related to the microstructure, indicating that the average chord length defines the size scale of the fracture profile (surface).

## HEIGHT DISTRIBUTIONS

The height distributions, as referred to the dividing line, must be symmetrical provided the measured results are statistically assured and the macroscopic load geometry is invariant. Measurements on single-phase ferrite indicate Gaussian-shaped height distributions (fig. 8). Thus the standard mean height deviation $\bar{H}$ is a sufficient descriptor for the height deviations. As discussed above $\bar{H}$ is sensitive to the exact cut-off value in wavelength in the filtering procedure (Wasén et al. (8)). The fact that no natural cut-off wavelength in the Fourier spectrum exists reflects the stochastic character of the microstructure and of the crack events. The choice of cut-off value is therefore a matter of judging the relevance of the information gained. A necessity in the

experimental profile analysis is to achieve symmetry in the height distribution which could be followed by studying the gradual fading out of the skewness of the height distribution upon increasing the measuring statistics. The cut-off wavelength as well as the total length of analysis should be proportional to the grain size of the material. It shall be noted that the height distribution contains information both about the fracture element size (i.e. the distance between deflections in the fracture path) and the angular deviation of the crack.

## SPATIAL CHARACTERIZATION. FRACTAL ANALYSIS

The spatial properties of the fracture profile can be exploited in various manners. Recently fractal analysis and the concept of fractal dimension have been applied in quantitative fractography (e.g. Wright and Karlsson (22), Underwood and Banerji (23), Wasén and Karlsson (24)). This kind of analysis was originally developed in order to give some insight into the importance of measurement resolution (Wright and Karlsson (22)). In addition, attempts to relate the appearance of the fractal plot of fracture profiles to the underlying microstructure have been made (Coster and Chermant (6)). Theoretical approaches (Wright and Karlsson (22)) have been mainly concentrated on curves with self-similarity, while the experimental applications have been concerned with how the measured length of an irregular curve depends on the size of the measuring unit.

The measuring element may be designed in various ways (Wright and Karlsson (22)). A common procedure is to substitute the real line with a chain of chords with constant length $\eta$ (fig. 9). It is sometimes found (Wright and Karlsson (22), Underwood and Banerji (23)) that the estimated length of a line varies proportionately to some power of the measuring element so that

$$\ell = \ell_o \cdot \eta^{1-D} \qquad (7)$$

where D lies between 1 and 2. Lines with a single definable length are called fractal lines and D is the fractal dimension (fig. 9). Normalization allows the length $\ell$ to be replaced by the linear roughness index $R_L$ (Wright and Karlsson (22)).

Analysis of experimental fracture profiles, however, reveals that the fractal curve has a sigmoidal shape (Wright and Karlsson (22), Underwood and Banerji (23), Wasén and Karlsson (24)) and can therefore not be characterized by a single slope D. Instead D is a function of the step length $\eta$. This is illustrated in fig. 10 showing a sigmoidal fractal curve corresponding to the experimental fracture profile in fig. 2 (Wasén and Karlsson (24)). It is evident that the curve asymptotically approaches both the bottom line and the upper level $\log(R_L^o)$ corresponding to the linear roughness index at full resolution. The shape of the curve seems fairly

symmetric around an inflection point situated at half height. This apparent symmetry around the inflection point at half height makes the coordinates of that point $(\log(\eta_{ip}), \log(R_L^o)/2)$ and a corresponding slope $(1-D_{ip})$ suitable as descriptors of the fractal curve.

Computer simulations (Wasén and Karlsson (24)) have shown that $D_{ip}$ is linearly dependent on the angle variance $\overline{\theta}_L^2$ of the fracture surfaces. Further the sideways position of the fractal curve as described by the abscissa in the inflection point $\log(\eta_{ip})$ (fig. 10) turned out to be linearly dependent on the size scale of the mean projected fracture element size $\overline{l}'$ $(= \overline{l}/R_L^o)$. The proportionality factors in these relations are determined by the spatial character of the fracture surface (Wasén and Karlsson (24)).

It has been shown that the over all appearance of the fractal curve can be mathematically described by the following general equation (Wasén and Karlsson (24)):

$$\log[R_L(\eta)] = [\log(R_L^o)/2]\cdot\{1-\tanh[\log(\eta/\eta_{ip})^{\beta}]\} \qquad (8)$$

where $\beta$ is a constant determined by the spatial character of the fracture surface. This equation with $\beta$=1.217 (cf. Wasén and Karlsson (24)) is indicated by the full line in fig. 10. By differentiation of eq. (8) a general expression for the "resolution" dependent $D(\eta)$ directly follows:

$$D(\eta) = 1+[\log(R_L^o)/2]\cdot\{\beta/\cosh^2[\log(\eta/\eta_{ip})^{\beta}]\} \qquad (9)$$

This allows an alternative formulation of the general regression formula 8:

$$\log[R_L(\eta)] = [(D_{ip}-1)/\beta]\cdot\{1-\tanh[\log(\eta/\eta_{ip})^{\beta}]\} \qquad (10)$$

i.e. the whole fractal curve is determined if the following characteristics of the fractal curve is known: the abscissa of the inflection point $(\eta_{ip})$, the slope of the fractal curve in the inflection point $D_{ip}$ and the constant $\beta$. Further, these parameters can be interpreted in basic geometrical quantities of the fracture surface as follows: $\eta_{ip}$ defines the "size scale", $D_{ip}$ is given by the angular properties and $\beta$ reflects the spatial characteristics of the fracture surface (Wasén and Karlsson (24)).

## EXPERIMENTAL APPLICATIONS OF QUANTITATIVE FRACTOGRAPHY

The topography of fatigue fracture surfaces has been studied by the quantitative profile analysis technique described above in a number of investigations (Wasén et al. (18), Hamberg et al. (14), Wasén et al. (25), Wasén and Karlsson (26)). The crack length measured was in all cases larger than a distance corresponding to

400 grain intercepts and thus sufficient for good averaging of the height distribution obtained after filtering. For the microstructures tested the standard mean deviation of height represents a mean value over the whole crack profile measured. The cracks were run at $\Delta K$-levels from the fatigue crack growth threshold to $\Delta K \approx 20$ MNm$^{-3/2}$, but no significant influence of the $\Delta K$-level was found in any case.

## Influence of grain size on fracture surface roughness

For single phase ferrite there is a linear relationship between the standard mean deviation of height $\bar{H}$ and the mean intercept grain size $\lambda$, fig. 11 (Wasén et al. (18)). Fig. 11 indicates that the meandering of the crack tip around the dividing line is in general confined to the width of one grain. However, the sideways movement of the crack tip in relation to the grain size is smaller in the coarser structures as the ratio $\bar{H}/\lambda$ decreases with increasing $\lambda$ (fig. 12) (Wasén and Karlsson (26)). The standard deviation of the angular distribution $\bar{\theta}_L$ in single phase ferrite is on the other hand mainly unaffected by the grain size, and has been shown to be $\approx 35^o$ (Wasén et al. (18)). Pearlite exhibits similar relations between the size of the microstructural unit (the colony) and $\bar{H}$, but with significantly smaller angular deviations with $\bar{\theta}_L \approx 15^o$ (Hamberg and Karlsson (27)).

## Influence of two-phase microstructures on fracture surface roughness

Which of the microstructural features that control the surface roughness is a matter of controversy. The size of the microstructural unit has been suggested as the prime factor (Wasén et al. (8), Wasén et al. (18), Hamberg and Karlsson (27), Suresh and Ritchie (28), Gray et al. (29)), and this view is convincingly supported for the "single" phases ferrite (Wasén et al. (28)) and pearlite (Hamberg and Karlsson (27)). In cases of more than one microstructural constituent, the stress field at the crack tip interacts with a phase mixture being plastically heterogeneous. This makes it more difficult to define a relevant microstructural unit. With introduction of a harder second constituent (pearlite or martensite) in a ferritic matrix, $\bar{H}$ may be expected to depend on both the crack retarding capacity and the volume fraction of the second phase relative to that of ferrite. In addition the grain size itself might influence as $\bar{H}/\lambda$ in the ferrite depends on $\lambda$ (fig. 12).

In coarse microstructures the height deviation $\bar{H}$ increases at increasing volume fraction of a harder second phase (at least as long as the ferritic phase is continuous) (Hamberg et al. (14)). The reason for this behaviour is that the advancing crack partly circumvents the harder constituent. As $\bar{H}/\lambda$ is relatively small in

pure, large-grained ferrite, this circumventing of the inclusions causes large deviations of the propagating crack in a phase mixture (fig. 12). At smaller grain sizes the relative crack deflection ($\bar{H}/\lambda$) in ferritic samples is larger (fig. 12). Introduction of inclusions will then cause less change of the crack topography. At very fine grained ferritic structures ($\lambda < 5$ $\mu$m) $\bar{H}$ approximately equals the grain size (i.e. $\bar{H}/\lambda \approx 1$), fig. 12, and additions of even martensite inclusions will not cause any further increase of the fracture surface roughness (Wasén and Karlsson (26)).

## Crack closure

The crack closure level increases with increasing roughness of the fracture surface (Wasén et al. (18), Hamberg et al. (14)). In fig. 13, $K_{cl}$ and $\bar{H}$ from a large number of investigations are collected (Wasén et al. (18), Hamberg et al. (14), Wasén et al. (25), Wasén and Karlsson (26)). With a reasonably small scatter the data fit a relation earlier developed for single phase ferrite (Wasén et al. (18)):

$$K_{cl} = 1.20 \cdot \bar{H}^{1/3} \quad (K_{cl} \text{ in } MNm^{-3/2} \text{ and } \bar{H} \text{ in } \mu m) \qquad (11)$$

This equation predicts that the crack closure level $K_{cl}$ in steels is determined by the roughness as defined by the well-defined standard height deviation $\bar{H}$ (note that $\bar{H}$ contains complex information about both the fracture element size and the angular deviation of the crack). Relation (11) is statistically very secured with a span of $\bar{H}$-values of approximately a factor 30 (cf. fig. 13).

The highest closure values are found in coarse microstructures with second phase inclusions close to being continuous and hard enough to cause a crack tip deflection (Hamberg et al. (14)).

## CONCLUDING REMARKS

The fracture surface created by running fatigue cracks has a stochastic character requiring statistical descriptions with distributions. Frequently the distributions are simple and can be described by mean values and standard deviations. The following descriptors have been shown to be effective:

1. Angle distributions. They are often Gaussian shaped around the main crack directions. The linear angle distributions can in many cases be converted to surface angle distributions. Roughness indices can be sometimes be used as alternatives to the mean standard deviation of the linear angle distribution.

2. Length distributions of chords approximating the true fracture profile. In single phase materials these distributions - like the grain intercepts - are found to be log-normally distributed.

3. Height distributions. They are simple to record and are very effective for predictions of, for instance, the crack closure. The height distributions are related to the angle and chord length distributions.

4. Spatial chararcterization. The Fourier spectrum and the fractal curve reflect similar properties of the fracture surface. The fractal curve and the fractal dimension are related to the linear roughness index.

The stochastic character of the fracture surface invalidates a regular modelling and measurement techniques relying on such simplifications. Experimental recordings of the fracture geometry generally requires filtering.

## REFERENCES

(1) Bauer, B., and Haller, A., Prakt. Metallogr., Vol. 18, 1981, pp. 327-341.

(2) Paul, J., Exner, H.E., Fripan, M., and Mehlo, H., Acta Stereol., Vol. 5/2, 1986, pp. 127-131.

(3) Wright, K., and Karlsson, B., J. Microscopy, Vol. 130/1, 1983, pp. 37-51.

(4) Banerji, K., and Underwood, E.E., Acta Stereol., Vol. 2/1, 1983, pp. 65-70.

(5) Underwood, E.E., Quantitative Stereology, Addison-Wesley, Reading, 1970.

(6) Coster, M., and Chermant, J.L., Intern. Metals Reviews, Vol. 28, 1983, pp. 228-250.

(7) Park, D.H., and Fine, M.E., In "Fatigue Crack Growth Threshold Concepts". Edited by D. Davidson and S. Suresh, AIME, New York, 1984, pp. 145-161.

(8) Wasén, J., Karlsson, B., and Hamberg, K., Acta Stereol., Vol. 6/1, 1987, pp. 199-204.

(9) Wasén, J., and Karlsson, B., 1988, to be published.

(10) Bengtsson, S., Johannesson, B., and Warren, R. In "Structure and crack propagation in brittle matrix composite materials" Edited by A.M. Brandt and I.H. Marshall, Elsevier Appl. Sci. Publ. Ltd, 1986, pp. 69-80.

(11) Karlsson, B., Wasén, J., and Hamberg, K., Fatigue '87, Proc. 3rd Intern. Conf. Fatigue, EMAS, Warley, 1987, pp. 1479-1492.

(12) Davies, P.W., and Wilshire, B., J Inst. of Metals, Vol. 90, 1962, pp. 470-472.

(13) Scriven, R.A., and Williams, H.D., Trans. AIME, Vol. 233, 1965, pp. 1593-1602.

(14) Hamberg, K., Wasén, J., and Karlsson, B., Fatigue '87, Proc. 3rd Intern. Conf. Fatigue, EMAS, Warley, 1987, pp. 135-144.

(15) Bertilsson, I., and Karlsson, B., Fatigue '87, Proc. 3rd Intern. Conf. Fatigue, EMAS, Warley, 1987, pp. 577-586.

(16) Underwood, E.E., Acta Stereol., Vol. 6/3, 1987, pp. 855-876.

(17) Underwood, E.E., J. Metals, Vol. 38, 1986, pp. 30-32.

(18) Wasén, J., Hamberg, K., and Karlsson, B., Mater. Sci. Engin., 1988, in print.

(19) Hamberg, K., Ph.D. Thesis, Chalmers Univ. Tech., Göteborg, Sweden, 1986.

(20) Sigl, L.S., and Exner, H.E., Metall. Trans. A, Vol. 18A, 1987, pp. 1299-1308.

(21) Woodhead, J.H., Prakt. Metallogr., Special issue 5, 1975, pp. 265-276.

(22) Wright, K., and Karlsson, B., J. Microscopy, Vol. 129/2, 1983, pp. 185-200.

(23) Underwood, E.E., and Banerji, K., Mater. Sci. Engin., Vol. 80, 1986, pp. 1-14.

(24) Wasén, J., and Karlsson, B., Proc. 8th Intern. Conf. Strength Metals and Alloys, Pergamon Press, 1988, in print.

(25) Wasén, J., Engström, E.U., and Karlsson, B., Proc. Stainless Steels '87, The Institute of Metals, 1988, in print.

(26) Wasén, J., and Karlsson, B., 1988, to be published.

(27) Hamberg, K., and Karlsson, B., this conf..

(28) Suresh, S., and Ritchie, R.O., In "Fatigue Crack Growth Threshold Concepts". Edited by D. Davidson and S. Suresh, AIME, New York, 1984, pp. 227-261.

(29) Gray, G.T., Williams, J.C., and Thompson, A.W., Metall. Trans. A, Vol. 14A, 1983, pp. 421-433.

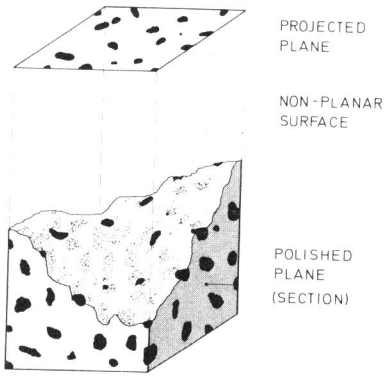


Fig. 1

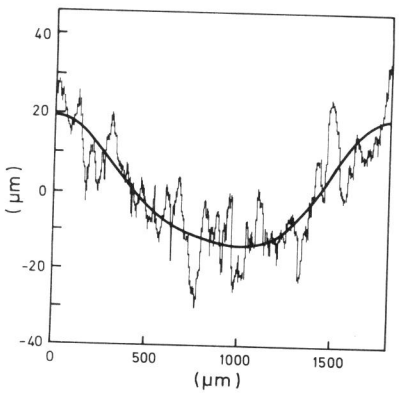


Fig. 2

Fig. 1 Main surfaces encountered in quantitative fractography.

Fig. 2 Experimental fatigue fracture profile. Single phase ferrite; mean intercept length $\lambda$ = 15 $\mu$m. Smooth curve defines the dividing line attained by filtering.

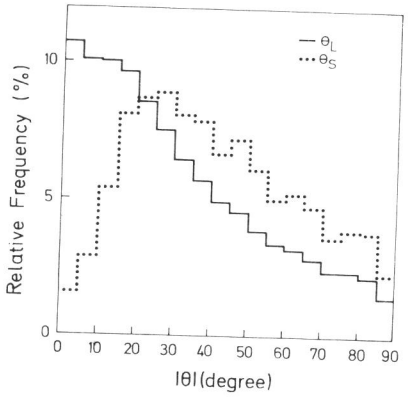


Fig. 3

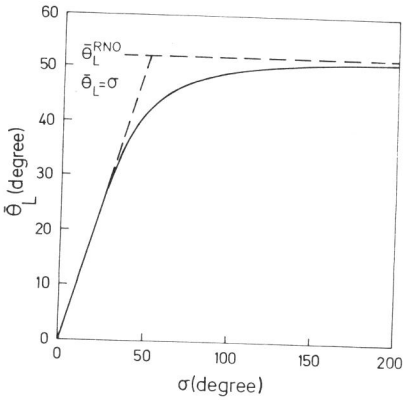


Fig. 4

Fig. 3 Experimental linear angle distribution $f(\theta_L)$ and areal angle distribution $g(\theta_S)$. Material as in fig. 2.

Fig. 4 Relation between the generating parameter $\sigma$ and the standard deviation $\bar{\theta}_L$ in eqs. 1a and 1b.

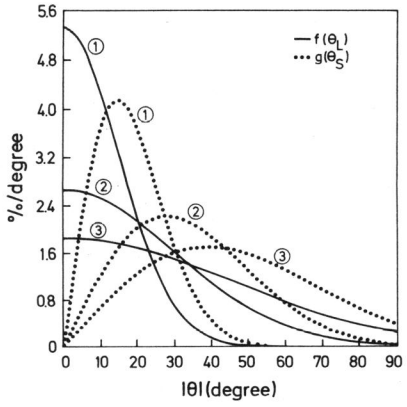


Fig. 5

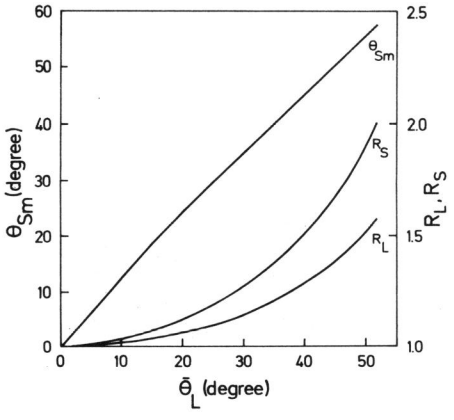


Fig. 6

Fig. 5 Theoretical linear angle distributions $f(\theta_L)$ (eq. 1a) and corresponding areal distributions $g(\theta_S)$. $\bar{\theta}_L = 15^o$ (no. 1), $30^o$ (no. 2) and $40^o$ (no. 3).

Fig. 6 Mean areal angle distribution ($\theta_{Sm}$) and roughness indices $R_S$ and $R_L$ vs. the standard deviation of the linear angle distribution $\bar{\theta}_L$ (eq. 1b).

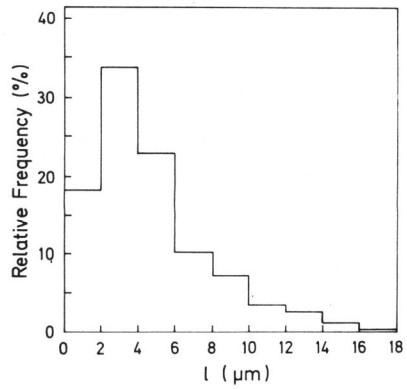


Fig. 7

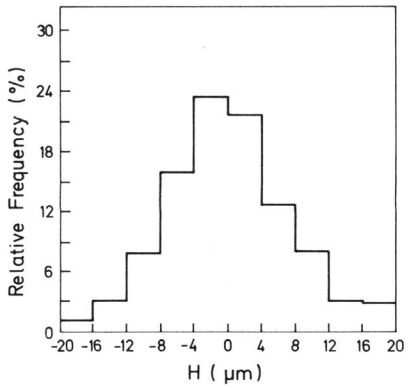


Fig. 8

Fig. 7 Size distribution of chords l approximating the fracture profile in fig. 2.

Fig. 8 Experimental height distribution. Material as in fig. 2. Filtered profile.

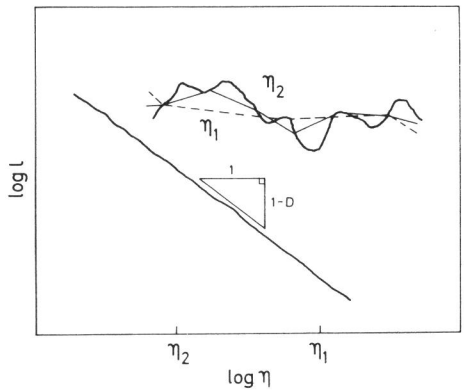


Fig. 9. Fractal plot of a curved line. For a true fractal the log 1 - log $\eta$ line is straight and unlimited.

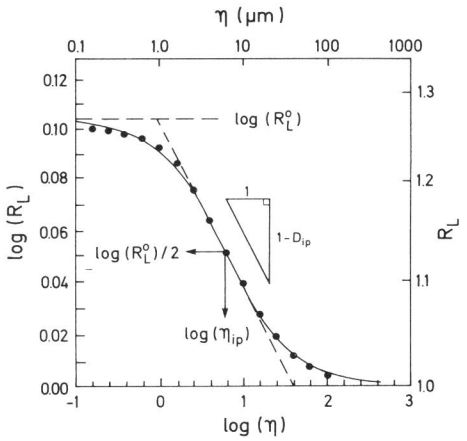


Fig. 10. Experimental fractal curve of the fracture profile in fig. 2. Full line represents prediction by eq. 8.

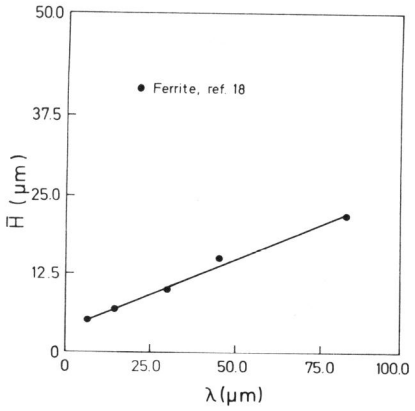


Fig. 11

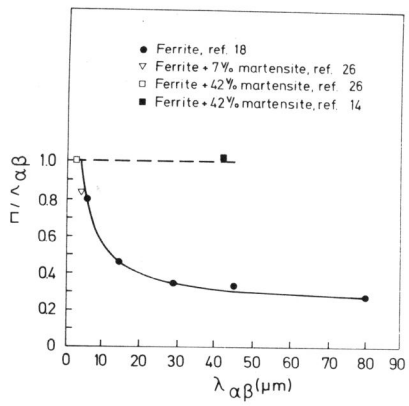


Fig. 12

Fig. 11. Mean standard deviation of height $\bar{H}$ vs. the mean linear intercept grain size $\lambda$ for single-phase ferritic steels.

Fig. 12. Relative crack deflection $\bar{H}/\lambda$ vs. the mean linear intercept grain size for single-phase ferritic and dual-phase ferritic/martensitic steels.

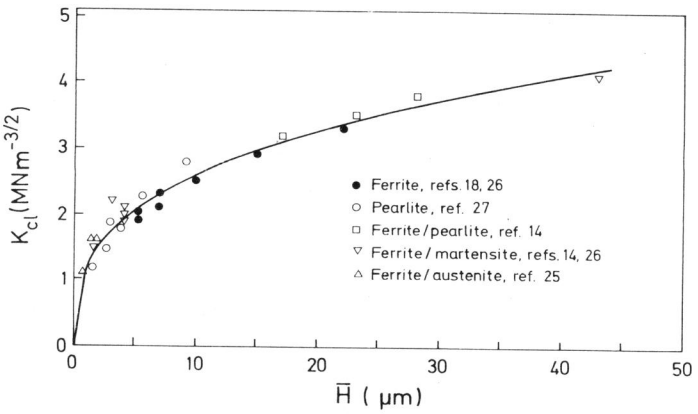


Fig. 13. Crack closure stress intensity $K_{cl}$ vs. the mean standard deviation of height $\bar{H}$. Full line shows the prediction by eq. 11.